ENVIRONMENTAL RESEARCH
COMMUNICATIONS

LETTER • OPEN ACCESS

Frequency of a state of cloud systems over tropical warm ocean

To cite this article: Shailendra Kumar and G S Bhat 2019 *Environ. Res. Commun.* **1** 061003

Environmental Research Communications

LETTER

Frequency of a state of cloud systems over tropical warm ocean

Shailendra Kumar[1,2] and G S Bhat[1]

[1] Centre for Atmospheric And Oceanic Sciences, Indian Institute of Science, Bengaluru, India
[2] Geophysical Institute of Peru, Lima

E-mail: shailendrak89@gmail.com

OPEN ACCESS

RECEIVED
18 February 2019

REVISED
10 June 2019

ACCEPTED FOR PUBLICATION
21 June 2019

PUBLISHED
1 July 2019

Keywords: remote sensing, cloud life cycle, convective area fraction, TRMM, tropical ocean

Supplementary material for this article is available online

Abstract

The knowledge of how long a mesoscale convective system stays in a given stage of life cycle is an important information for many practical applications. A unique approach has been adopted here to find the stage of development of convective cloud systems (CCSs) over tropical oceanic areas. We use the Tropical Rainfall Measuring Mission (TRMM) data products, and define a cloud system (CS) based on criteria that depend on TRMM precipitation radar equivalent radar reflectivity factor (Z_e) and TRMM Microwave Imager polarization corrected temperature data. Average vertical profile of Z_e and convective area fraction (CAF) of a CS are used to identify its state which is a proxy for life stage. We use two parameters, namely reflectivity differences (RD) and convective area fraction (CAF) and defined 5 states of CS life cycle. Our results show that majority of CSs are found in mature stage and formative and dissipation stages are relatively short over the twelve warm tropical oceanic areas selected for analysis. Each ocean has a distinct signature in the RD-CAF phase space, and, there are regional/seasonal differences within an ocean basin. Bay of Bengal has less CAF compared to the equatorial Indian ocean. In the tropical Pacific Ocean, majority of the CSs lie in mature stage with CAF between 0.3 to 0.6, whereas, CSs in mature stage over the Atlantic Ocean have their CAF between 0.2 and 0.3. CS characteristics over the Atlantic Ocean during the Boreal summer and winter are different.

1. Introduction

Typical life span of a mesoscale convective system (MCS) is from a few hours to less than a day with its life cycle consisting of formative, intensifying, mature and dissipating stages (Leary and Houze 1979). The knowledge of how long an MCS stays in a given life stage is an important information because atmospheric response to convective heating depends on the vertical profile of heating (Webster and Stephens 1984, Randall *et al* 1989) which depends on MCS life stage (Leary and Houze 1979, Houze 1982). Horizontal and vertical distributions of equivalent radar reflectivity factor (Z_e) measured by a weather radar are often used to identify an MCS and its life stage (Leary and Houze 1979). Spatial coverage of ground mounted weather radars is very limited and only those mounted on board satellites can provide global distribution of Z_e. In particular, data collected with payloads on board the Tropical Rainfall Measuring Mission (TRMM) satellite (Kummerow *et al* 1998) have revolutionized our understanding of tropical precipitating cloud systems (e.g., Zipser *et al* 2006, Houze *et al* 2015). With the TRMM revisit time of at least several hours, its data products are not ideally suitable for the study of life cycle of MCSs. Despite this limitation, a few attempts have been made in the past to obtain aspects of life stage of MCSs using the TRMM data. Kondo *et al* (2006) investigated the relationship between the evolution stage of MCSs and collocated TRMM precipitation parameters over the Maritime Continent and the Western Pacific Ocean. They observed that irrespective of life duration and location of cloud systems, individual cloud systems exhibit some common features, namely, minimum blackbody brightness temperature (T_B), size of cold area and T_B gradient at cloud edges in the beginning stage of cloud systems. Futyan and Del Genio (2007) compared life cycle of MCSs over Africa using the TRMM Precipitation Radar (TRMM-PR) and the Lightning Imaging Sensor (LIS) data, and

observed fundamental differences in their life cycle over land and oceans. Imoka and Nakamura (2012) studied different stages of evolution of tropical cold cloud systems over the Maritime Continent and a part of the tropical Western Pacific using *Multifunctional Transport Satellite*-1*R* (MTSAT-IR) and TRMM-PR data. They divided cold cloud systems life cycle into 1 h to 5 h and studied the vertical profiles of convective and stratiform rainfall within different stages of evolution. The longer-lived cloud systems show bigger anvil area, whereas short lived systems decay rapidly and do not produce extensive cloud cover and precipitation.

Past literature does not tell if there is preference for MCSs to stay more frequently in a given stage of life cycle in some regions or all areas show similar behaviour. A study by Houze *et al* (2015) alludes to it in the passing. The main objective of this study is finding an answer to this question using the TRMM data. The paper is organized as follows. Section 2 discusses the data and methods, section 3 results and section 4 contains discussion and section 5 conclusions.

2. Data and methods

2.1. TRMM PR and TMI

TRMM product 2A25, the TRMM-PR measured and attenuated-corrected equivalent radar reflectivity factor (Z_e, version 6, e.g., Iguchi *et al* 2000) is the main data used. Detailed technical specifications of the TRMM-PR can be found in Kummerow *et al* (1998) and important points relevant to this work are only listed below. The TRMM is a non-polar orbiting satellite and its revisit time is a function of latitude and time (Negri *et al* 2001) with a maximum frequency of ~8 per day. The horizontal and vertical resolutions of the TRMM-PR at nadir are ~5 km × 5 km and 0.25 km, respectively (after the TRMM orbit boost in August 2001). We corrected for the altitude of TRMM-PR beams to get the correct height above the Earth ellipsoid as described in Bhat and Kumar (2015), since the TRMM-PR vertical levels of inclined beams do not correspond to local height. The TRMM-PR data processing algorithm has omitted data of pixels with Z_e below 15 dBZ at the processing stage itself (Kummerow *et al* 1998). We use TRMM 2A23 product for the convective-stratiform rain classification (Awaka *et al* 1997). TRMM Microwave Imager (TMI) 1B11 data is used for the polarization corrected temperature (PCT; Spencer *et al* 1989, Nesbitt *et al* 2006). A PCT threshold of 250 K is used to identify deep convective clouds. TRMM 3B42 data is taken for precipitation (Huffman *et al* 2007) and sea surface temperature (SST) is from AMSRE (Gentemann *et al* 2010).

We report results mainly for oceanic regions in the following. Since SST has a pronounced influence on convection and precipitation over the tropical oceans (e.g., Gadgil *et al* 1984, Graham and Barnett 1987, Waliser and Graham 1993), twelve oceanic areas with high seasonal SSTs and precipitation are selected (figures 1(a), (b)). The results are based on a ten-year climatology (2001–2010) and include two seasons, namely, June to September (JJAS) and January to March (JFM). Geographic location and spatial extents of the study areas are given in table 1. Areas selected include the Bay of Bengal, Maritime continent, tropical Indian, Pacific and Atlantic oceans. Detailed justification for each area can be found in Kumar and Bhat (2016) and here discussed in brief for some of the areas. 'Maritime Continent' (MC) is one of the rainiest regions on the planet (Ramage 1968) and considered for both the seasons. The head of the Bay consists of deep convective clouds throughout the summer monsoon season (Bhat *et al* 2001) and higher frequency of intense clouds compared to Arabian sea (Bhat and Kumar 2015, Kumar 2017a). Atlantic Ocean has higher fraction of shallow convection during JJAS months (Kumar 2018) and fewer deeper and intense convection during JFM months (Kumar 2017b, Kumar *et al* 2019).

2.2. Cloud system (CS)

In this work, a cloud system (CS) is defined as a set of connected pixels in the two-dimensional projection of columnar maximum Z_e with the total area of connected pixels >500 km^2. In any given population of CSs, small sized CSs outnumber the large sized CSs (Liu and Zipser 2015, Kumar 2016, Kumar *et al* 2019), however, the larger ones matter more for total precipitation (Houze 2004, Liu and Zipser 2015, Kumar *et al* 2019). A large sized CS also has relatively a small area during its formative stage, identification of which is important for our objective. The minimum area of a CS is so chosen as to have a balance between missing out CSs during their formative/intensifying stage versus including too many small systems in the analysis. One of the limitations of the TRMM-PR is that its swath is ~250 km and it is possible that the TRMM-PR saw a small portion of a large CS. To partially overcome this limitation, we considered simultaneous PCT data. The swath of TMI is three times that of the TRMM-PR, and its PCT can indicate the overall spatial extent of a cloud system seen by the TRMM-PR (e.g., figure 2). In order to avoid a portion of a large cloud system being treated as a CS, a condition on common area overlap between the TRMM-PR and TMI PCT (with a threshold of 250 K) is imposed. A CS is included in subsequent analysis if its area detected in the Z_e projection is at least 50% of its area seen in the PCT imagery.

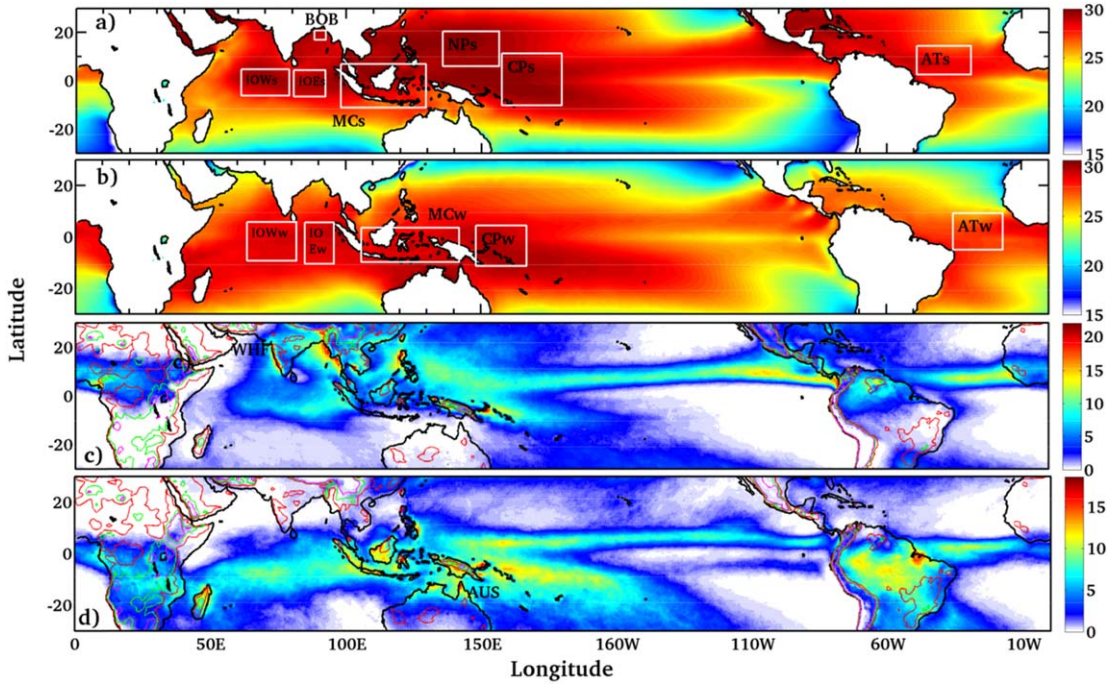

Figure 1. Seasonal average SST and precipitation considering the ten-year period from 2001 to 2010. TMI SSTs and TRMM 3B42 rainfall products are shown. (a) SST, June to September; (b) SST, January to March; (c) June to September daily average precipitation; and (d) January to March daily average precipitation. Color bars on right show SST in degree Celsius and precipitation in mm day^{-1}. Areas selected for detailed analysis are shown by rectangular boxes.

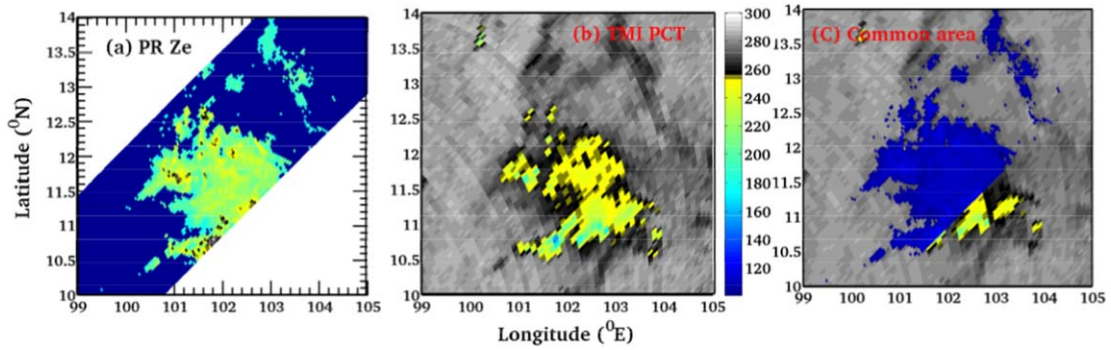

Figure 2. An example of simultaneous TRMM-PR and TMI PCT measurements. (a) Projection of maximum reflectivity of the TRMM-PR. (b) TMI PCT. (c) Common overlapping area between the TRMM-PR and TMI PCT is shown in the blue color.

Table 1. Boundary and number of cloud systems used in the present study.

Regions	Boundary Season	Number of Cloud systems
Bay of Bengal (BOB)	15 °N–19 °N, 86°–93 °E; JJAS	1271
Indian Ocean west (IOWs)	5 °S–3 °N, 55°–79 °E; JJAS	2019
Indian Ocean east (IOEs)	5 °S–3 °N, 81°–100 °E; JJAS	2008
Maritime Continent (MCs)	9 °S–10 °N, 105°–130 °E; JJAS	2760
North Pacific (NPs)	5°–20 °N, 135°–155 °E; JJAS	3469
Central Pacific (CPs)	15 °S–5 °N, 156 °E–170 °W; JJAS	3488
Atlantic Ocean (ATs)	0°–10 °N, 20°–50 °W; JJAS	2713
Indian Ocean west (IOWw)	10 °S–2 °N, 55°–79 °E; JFM	1698
Indian Ocean east (IOEw)	11 °S–2 °N, 87°–95 °E; JFM	1882
Maritime Continent (MCw)	12 °S–0°, 110°–140 °E; JFM	3728
Central Pacific (CPw)	11 °S–2 °N, 145 °E–170 °W; JFM	2115
Atlantic Ocean (ATw)	3 °S–7 °N, 10°–30 °W; JFM	1715

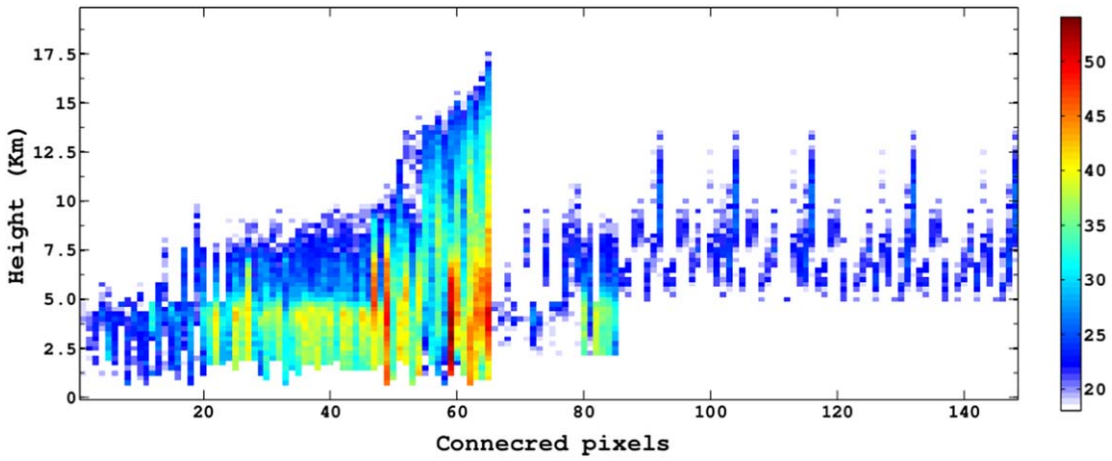

Figure 3. An example of a CS captured by the TRMM-PR on 01 June 2003. Each connected beam within the projected area of the CS is given a number starting with the left most column in the lowest row along the track and then the row above, and so on. The unit of color bar is in dBZ.

Figure 3 shows one example of vertical structure of a CS constructed from the TRMM-PR data. Those beams with their Z_e extending below 2.5 km level correspond to convective part (i.e., contains Cb and cumulus congestus clouds) of the CS. There are several beams with their base height above 5 km. These belong to the anvil cloud part of the CS. The overall vertical structure of the beams resembles that of a MCS in mature stage (Leary and Houze 1979).

2.3. State of a CS

The major assumption of this work is that life stage of a CS is reflected in the average vertical profile of its Z_e field (Leary and Houze 1979, Szoke and Zipser 1986, Williams and Houze 1987, Mapes and Houze 1993, Chen and Houze 1997). Figure 4 shows six examples of average vertical profiles of CSs over the Bay of Bengal box derived from the TRMM-PR data. Major differences are observed in the shape of these profiles below 6 km. For example, for CS1, Z_e increases towards the surface and the maximum Z_e occurs at the lowest level shown. In the case of CS2, average Z_e is higher between 2 and 5 km compared to CS1, its Z_e increases towards the surface, however, increase in the layer of the atmosphere below 4 km is less compared to that of CS1. CS4 has the highest Z_e between 2 and 5 km compared to other profiles with the maximum at 4.5 km. Level of the zero-degree Celsius isotherm is around 530 hPa (corresponds to 5–5.5 km altitude) over the Bay of Bengal during summer (e.g., Bhat 2002). The sharp increase in Z_e of CS4 at 4.5 km is a clear indication of the formation of a bright band. Profile of CS5 is nearly identical to that of CS4 above 4.5 km, however, has smaller Z_e values in the lower troposphere. CS6 shows a bright band but is less intense compared to CS4 and CS5. Ground radar observations have shown that average vertical profiles showing highest Z_e near 2 km are dominated by convective rainfall (e.g., figure 11 of Imoka and Nakamura 2012), whereas, peak near the melting level is owing to dominance of stratiform precipitation with bright band (e.g., figure 12 of Imoka and Nakamura 2012). Therefore, profiles shown in figure 4 represent CSs in different stages of development. For example, CS4 is in mature stage, CS3 in early mature stage, and CS6 in the dissipating stage. CS1 and CS2 are that of a CS in formative intensifying stages, respectively.

Thus, average vertical Z_e profile of a CS contains information about its life stage. As a CS transitions from intensifying to mature stage, bright band develops and its maximum Z_e shifts from the lower troposphere to the bright band level (figure 4). Therefore, difference in the average Z_e between the lower troposphere and around bright band level acts as a proxy for the stage of development of a CS. Taking the average Z_e profile of a CS, we define a parameter RD (reflectivity difference) as,

$$RD = Z_{mb} - Z_{ll} \quad (1)$$

where Z_{mb} is the maximum value of Z_e between 4 and 6 km (i.e., melting band region) and Z_{ll} is the maximum value of Z_e between 1.5 and 3 km (i.e., low level). Values of RD mostly lie in −5 dBZ to +5 dBZ range with more number of occurrences between −2 and 2 dBZ (supplementary figure S1 is available online at stacks.iop.org/ERC/1/061003/mmedia). Frequency distribution of RD shows nearly continuous variation with no hints to delineate life stages. Therefore, we explored other proxies and aimed to identify the life stages in a two dimensional phase space. Area of a CS during the initial and decay stages are dominated by convective and stratiform precipitation, respectively. Therefore, convective area fraction (CAF) is another indicator of the life stage of a CS. Here, CAF of a CS is defined as,

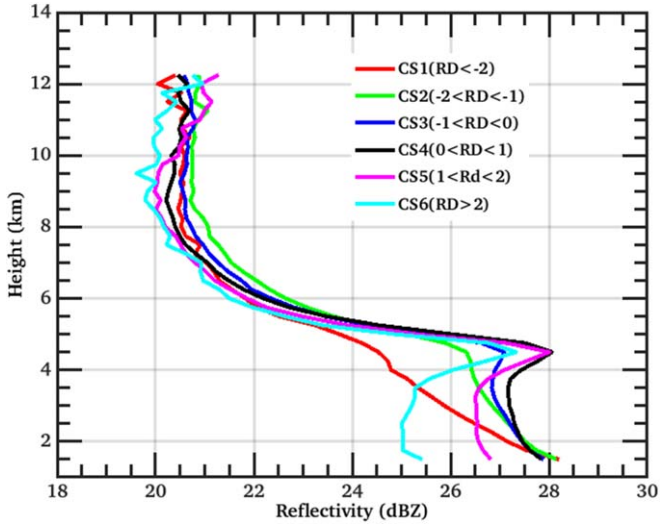

Figure 4. Average vertical profiles of CSs over the Bay of Bengal box. Number inside the brackets is RD in dBZ units. Average profile of CS represented by the red line shows highest Z_e values below 2 km, and the CS is in its formative stage. In profile A2 (green line), Z_e has increased between 4 and 6 km. This CS is in intensifying or approaching the early mature stage. In the profiles corresponding to the blue and black colored lines, maximum Z_e between 4 and 6 km has increased clearly indicating the presence of a bright band. Notice that the values of Z_e around 2 km height do not undergo any major change in the two profiles. These correspond to CS is mature stage. For the average profile of CS corresponding to the magenta color, Z_e remains high between 4 and 5 km while that at 2 km shows relatively a smaller value, i.e., average Z_e at lower levels is decreasing. This CS is past its prime and approaching the dissipating stage. For the average profile of CS in the cyan color, Z_e has decreased at 2 km height while higher Z_e prevails around the freezing level. This CS is in the dissipating stage.

$$\mathrm{CAF} = \mathrm{N_c}/\mathrm{N_T}, \tag{2}$$

where N_c is the number of TRMM 2A23 pixels within the CS area identified as convective, and N_T is the total number of PR beams in the CS. It is observed that major fraction of CAFs lie between 0.2 and 0.7 (e.g., supplementary figure S2).

3. Results and discussion

Figure 5 shows the frequency distribution of CSs in RD-CAF phase space (i.e., the probability of occurrence of different CS states) over twelve tropical oceanic areas. Here, number of occurrences in a grid box of size 1 dBZ $\times$ 0.1 in RD-CAF phase space is counted and then normalized by the maximum count among the grid boxes. Those grids having normalized occurrence of less than 10% are not plotted. The formative stage of a CS is characterized by negative RD and large CAF, while positive RD and small CAF characterize a CS in the dissipating stage. Thus, different regions in RD - CAF phase space correspond to different life stages of a CS and each grid represents a certain stage in the evolution of a CS. A grid in RD and CAF phase-space represents a 'CS state' in this work. After manually examining several cases belonging to different grids in figure 5 and assigning them to nearest MCS life stage, it was noted that it is primarily RD ranges that have close matching to life stages of MCSs (supplementary figure S3). In view of this, we have defined five states of CSs which approximately corresponds to different life stages of CSs (table 2). A CS in state S1 is likely to be in formative stage, that in state S2 intensifying, in states S3 and S4 in mature stage and in state S5 in dissipating stage (table 2).

Figure 5 summarizes the wide range of states in which a majority of tropical CSs exist over warm waters of tropical oceans. The most preferred state of CSs in a given area is the grid having the highest occurrence (i.e., 100%). The most preferred state in half of the areas studied, namely, BoB, IOWs, IOEw, MCw, ATs, ATw) is the grid 0–1 dBZ (RD) and 0.1–0.2 (CAF), i.e., CSs are most frequently found in the mature stage (table 2) in these areas. MCs and NPs show two preferred states, namely, -1 to 0 dBZ $\times$ 0.2 to 0.3 and, 0 to 1 dBZ $\times$ 0.1 to 0.2. Central Pacific box shows preference for intensifying stage, i.e., RD of -1 to -2 dBZ and, CAF of 0.3 to 0.4. Thus, formative and dissipating stages are of relatively short duration compared to that of the mature stage across the oceanic areas (table 2). Preferred CAFs vary between 0.1 to 0.2 and 0.3 to 0.4.

An important outcome of figure 5 is that each area exhibits a distinct distribution in RD-CAF space, and summer and winter distributions can be different over a given ocean basin, e.g., IOEs and IOEw. IOEs, CPs and CPw show a wide-spread distributions while IOEw is more compact. Differences in RD and CAF imply differences in the vertical distribution of hydrometeors and in the vertical profile of heating, respectively. Thus, figure 5 shows that CSs over warm tropical oceans are not identical and there are region specific preferences for the duration they spend in a given

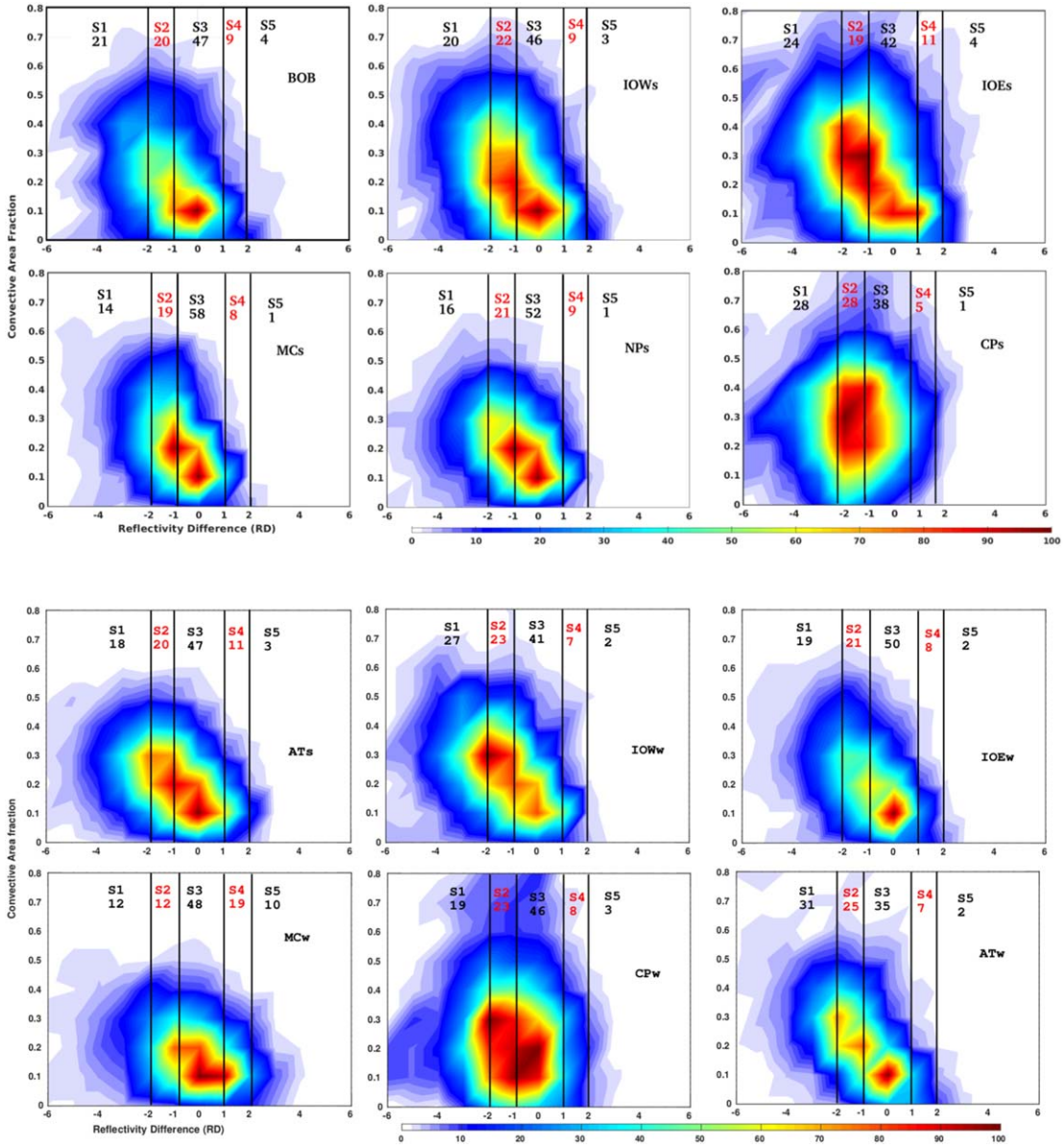

Figure 5. Frequency distribution of RD and CAF pairs in different areas over the tropical oceans. Values shown are number of occurrences in each bin normalized by the maximum number of data points among all the bins in respective areas and multiplied by 100. Bins with frequencies less than 10% are not shown. In each panel, S1, S2, etc, refer to CS states (table 2) and the numbers below give the total frequency of occurrence of respective states.

Table 2. Identification of the state of a cloud system based on reflectivity difference (RD) and convective area fraction (CAF).

Number	RD	State	Approximate life stage
1.	RD $\leqslant -2$ dBZ	S1	Formative
2.	-2 dBZ $<$ RD <-1 dBZ	S2	intensifying and early mature
3.	-1 dBZ $<$ RD $<$ 1 dBZ	S3	Mature
4.	1 dBZ $<$ RD $<$ 2 dBZ	S4	Late mature and early dissipating
5.	RD $\geqslant$ 2 dBZ	S5	Dissipating

state. Even for a given state as defined in table 2, regional differences are observed in the vertical structure of CSs across the oceanic area which are brought out succinctly in the contoured frequency by altitude diagrams (CFADs; Yuter and Houze 1995) shown in figure 6. CFADs are constructed for different states based on the classification given in table 2. Average vertical profile of Z_e is also shown in respective CFADs. It is observed from figure 6 that average vertical profiles hide the subtle differences that exist among different areas. As expected, CSs in state S1 (figure 6(a)) show the highest width and more probability of highest Z_e between 2–3 km. Upward shift in the CFAD with increasing CS state

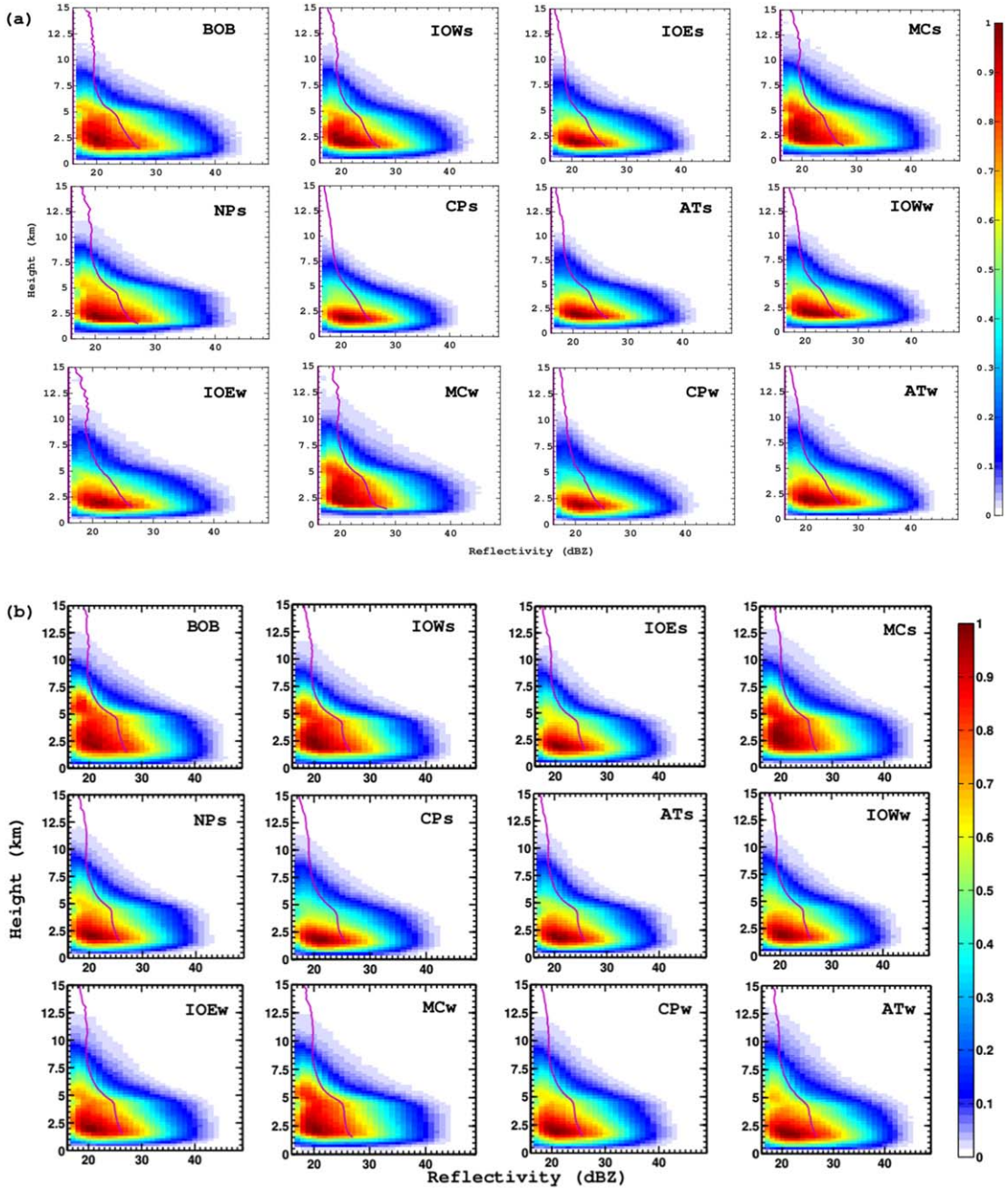

Figure 6. (a): CFAD of CSs in state S1 over different tropical oceanic areas. The continuous line shows the average of all CSs belonging state S1. (b): Same as 6a but for state S2. (c): Same as 6a but for state S3. (d): Same as 6a but for state S4. (e): Same as 6a but for state S5.

is seen in figure 6. Figure 6(b) shows the CFAD of CSs in state S2. Areas such as BOB, IOWs, MCs, IOEw, MCw show higher values of Z_e around 5 km altitude compared to the rest. CFAD of state S3 (figure 6(c)) shows two modes, one around 2.5 km and another between 5 and 6 km except for BOB. Bright band is well developed in all cases. Average Z_e is nearly constant below the freezing level and above the 8 km. CFAD of state S4 (figure 6(d)) shows further strengthening of the bright band. Probability of finding Z_e values above 35 dBZ has decreased considerably in state S5 (figure 6(e)) compared to state S4, its mode lies above the bright band, and the average extent of cloud top has decreased.

4. Discussion

To the best of our knowledge, the only previous study which attempted to link TRMM-PR data derived precipitating cloud structure to life stage of a CS is that of Houze *et al* (2015). Depending on the horizontal and vertical structure of connected pixels in the TRMM-PR data, they define deep convective core (DCC), wide

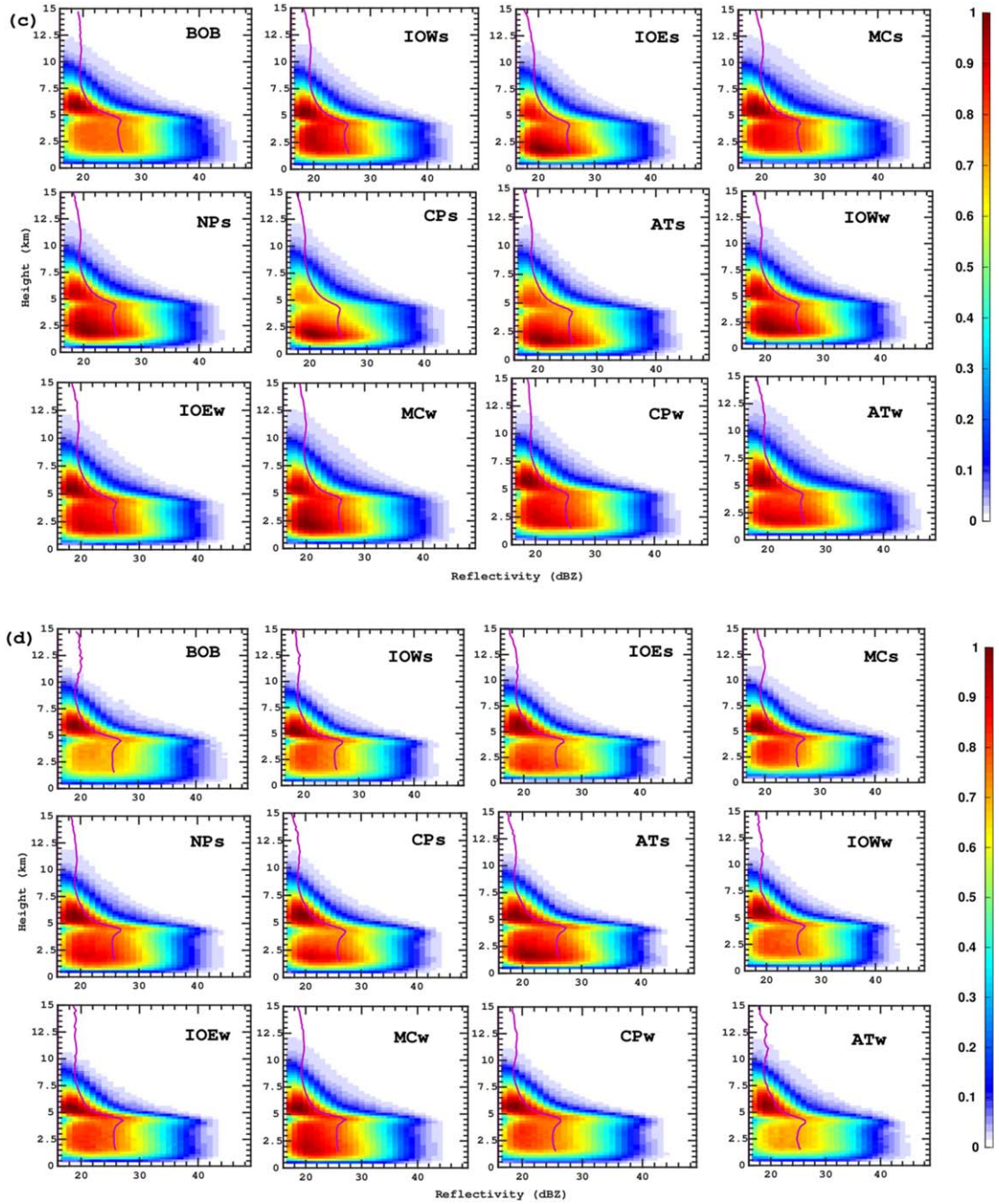

Figure 6. (Continued.)

convective core (WCC) and broad stratiform region (BSR), which resemble the early, middle, and late stages of MCSs. Relative frequency of occurrences of DCCs, WCCs and BSRs show strong spatial and seasonal differences, and wide variety of convective organization, e.g., robust stratiform precipitation and widespread cellular stratiform precipitation. Direct comparison of our and Houze *et al* (2015) works is not correct owing to fundamental differences in the definitions of the cloud systems in these works. In particular, we use 500 km^2 as the minimum area for a CS while smallest area of WCC is 800 km^2 at 30 dBZ threshold in Houze *et al* (2015).

If CSs follow the canonical MCS evolution, then we expect CS states to fall along a line from upper left corner (i.e., high CAF and more negative RD) to lower right corner (i.e., low CAF and more positive RD). There are hints of this in BOB, MCs, NPs, IOWw, IOWw, ATs and ATw boxes. There are also exceptions. For example, there are CSs with their CAF of less than 0.2 and RD<-4 dBZ (e.g., CPs and CPw boxes), i.e., the average profile is somewhat like that of CS1 in figure 4. Such a profile means that stratiform precipitation area is large, melting band is absent, i.e., these are not canonical type MCSs with a glaciated anvil. Then the associated stratiform region is perhaps primarily made of shallow or mid-level stratus clouds. Since CS contains pixels with

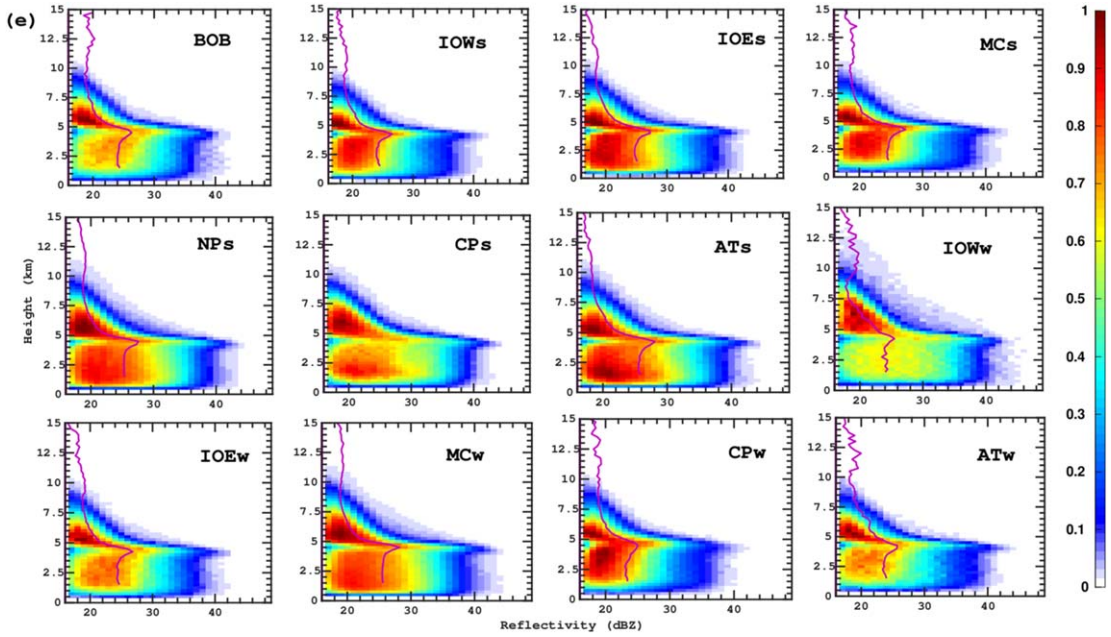

Figure 6. (Continued.)

PCT $\leqslant$ 250 K, it has ice phase and contains cold pixels also. Similarly, CSs with RD $>$ 3 dBZ and CAF $>$ 0.5 (e.g., IOEs), i.e., have a well-developed bright band region but more area occupied by convective clouds. Further analysis is needed to understand the structure of such CSs and under what conditions they form. Case studies by taking samples from different CS states in figure 5 will help in better understanding the spectrum of tropical precipitating systems.

In the absence of ground based or geostationary satellite data, it is not possible to observe the life stages of CSs. Based on the average vertical structure of Z_e and convection area fraction, we assigned a state to a CS (table 2) which is a proxy but not identical to the CS life stage. The most preferred or probable state resembles the vertical structure associated with mature stage of a MCS over all oceanic areas having the seasonal warmest SSTs. Our study also brings out possibility of region specific CS structures which are different from that of a canonical MCS. For example, there are not a negligible number of CSs which have low convective area fraction but average vertical structure similar to that of cumulus congestus clouds (i.e., large negative RD). This peculiar feature is observed over the Central Pacific Ocean and Equatorial Indian Ocean, in particular.

5. Conclusions

Following are the major conclusions from the study:

1. If CSs over tropical warm oceans are sampled randomly, they are most likely to be found in the mature stage.
2. Very rare to find CSs with convective area fraction of more than 60% over warm tropical oceanic areas.
3. Each ocean has a distinct signature in the RD-CAF phase space.

Acknowledgments

This work was partially supported with funds from the Ministry of Earth Sciences, Govt. India under the CTCZ program. Authors thank the Ministry for the support. TRMM 2A25 (http://mirador.gsfc.nasa.gov/cgi-bin/mirador/presentNavigation.pl?tree=project&dataset=2A25%20%28Version%20007%29:%20Radar%20Rainfall%20Rate%20and%20Profile%20%28PR%29&project=TRMM&dataGroup=Orbital& version=007) and 3B42 (http://mirador.gsfc.nasa.gov/cgi-bin/mirador/presentNavigation.pl?tree=project&dataset=3B42:%203-Hour%200.25%20×%200.25%20degree%20merged%20TRMM%20and%20other%20satellite%20estimates&project=TRMM&dataGroup=Gridded& version=007) data are taken from NASA's Earth–Sun

System Division website. The authors thank the anony- mous reviewers for their constructive suggestions. TMI data were produced by Remote Sensing Systems, Inc., and were sponsored by the NASA Earth Sciences Division.

ORCID iDs

Shailendra Kumar https://orcid.org/0000-0002-1442-7967

References

Awaka J, Iguchi T, Kumagai H and Okamoto 1997 KI Rain type classification algorithm for TRMM precipitation radar Ingeoscience and remote sensing, 1997 IGARSS'97 remote sensing-a scientific vision for sustainable development *1997 IEEE International* **4** 1633–5

Bhat G S *et al* 2001 BOBMEX - the Bay of Bengal monsoon experiment *Bull Amer Meteor Soc* **82** 2217–43

Bhat G S 2002 Near-surface variations and surface fluxes over the northern Bay of Bengal during the 1999 Indian summer monsoon *J. Geoph. Res. Atmosph.* **107**

Bhat G S and Kumar S 2015 Vertical structure of cumulonimbus towers and intense convective clouds over the South Asian region during the summer monsoon season *J. Geophys. Res.* **120** 1710–22

Chen S S and Houze R A 1997 Diurnal variation and life-cycle of deep convective systems over the tropical Pacific warm pool *Q. J. Roy. Meteorol. Soc.* **123** 357–88

Futyan J M and Del Genio A D 2007 Deep convective system evolution over Africa and the tropical Atlantic *J. Clim.* **20** 5041–60

Gadgil S, Joshi N and Joseph P 1984 Ocean-atmosphere coupling over monsoon regions *Nature* **312** 141

Gentemann C L, Wentz F J, Brewer M, Hilburn K and Smith D 2010 Passive microwave remote sensing of the ocean an overview *In Oceanography from Space* 13–33

Graham N and Barnett T 1987 Sea surface temperature, surface wind divergence, and convection over tropical oceans *Science* **238** 657–9

Houze R A 1982 Cloud clusters and large-scale vertical motions in the tropics *J. Meteorol. Soc. Japan* **60**

Houze R A 2004 Mesoscale convective systems *Rev. Geophys.* **42** RG4003

Houze R A, Rasmussen K L, Zuluaga M D and Brodzik S R 2015 The variable nature of convection in the tropics and subtropics: a legacy of 16 years of the tropical rainfall measuring mission satellite *Rev. Geophy.* **53** 994–1021

Huffman G J, Bolvin D T, Nelkin E J, Wolff D B, Adler R F, Gu G, Hong Y, Bowman K P and Stocker E F 2007 The TRMM multisatellite precipitation analysis (TMPA): quasi-global, multiyear, combined-sensor precipitation estimates at fine scales *J. Hydrometeorol.* **8** 38–55

Iguchi T, Meneghini R, Awaka J, Kozu T and Okamoto K 2000 Rain profiling algorithm for trmm precipitation radar data *Adv. Spc. Res.* **25** 973–6

Imaoka K and Nakamura K 2012 Statistical analysis of the life cycle of isolated tropical cold cloud systems using MTSAT-1R and TRMM data *Mont. Wea. Rev.* **140** 3552–72

Kondo Y, Higuchi A and Nakamura K 2006 Small-scale cloud activity over the Maritime Continent and the western Pacific as revealed by satellite data *Mon. Wea. Rev.* **134** 1581–99

Kumar S 2016 Three dimensional characteristics of precipitating cloud systems observed during Indian summer monsoon *Adv. Spc. Res.* **58** 1017–32

Kumar S 2017a A 10-year climatology of vertical properties of most active convective clouds over the Indian regions using TRMM PR *Theoretical Appl. Climatol.* **127** 429–40

Kumar S 2017b *Vertical Characteristics of Reflectivity in Intense Convective Clouds using TRMM PR Data Environment and Natural Resources Research* **7** 58

Kumar S 2018 Vertical structure of precipitating shallow echoes observed from TRMM during Indian summer monsoon *Theor. Appl. Climatol.* **133** 1051–9

Kumar S and Bhat G S 2016 Vertical profiles of radar reflectivity factor in intense convective clouds in the tropics *J. Appl. Meteorol. Climatol.* **55** 1277–86

Kumar S, Silva Y, Moya-Álvarez A S and Martínez-Castro D 2019 Seasonal and regional differences in extreme rainfall events and their contribution to the world's precipitation: GPM observations *Adv. Meteorol.* Article ID 4631609 15

Kummerow C, Barnes W, Kozu T, Shiue J and Simpson J 1998 The tropical rainfall measuring mission (trmm) sensor package *J. Atmos. Ocean Tech.* **15** 809–17

Leary C A and Houze R A 1979 The structure and evolution of convection in a tropical cloud cluster *J. Atmos. Sci.* **36** 437–57

Liu C and Zipser E J 2015 The global distribution of largest, deepest, and most intense precipitation systems *Geophys. Res. Lett.* **42** 3591–5

Mapes B E and Houze R A 1993 Cloud clusters and superclusters over the oceanic warm pool *Mon. Wea. Rev.* **121** 1398–416

Negri A J, Bell T L and Xu L 2001 Sampling of the diurnal cycle of precipitation using TRMM *J. Atmosph. Ocean. Tech.* **19** 1333–44

Nesbitt S W, Cifelli R and Rutledge S A 2006 Storm morphology and rainfall characteristics of TRMM precipitation features *Mon. Wea. Rev.* **134** 2702–21

Ramage C S 1968 Role of a tropical 'maritime continent' in the atmospheric circulation *Mon. Wea. Rev.* **96** 365–70

Randall D A, Dazlich D A and Corsetti T G 1989 Interactions among radiation, convection, and large-scale dynamics in a general circulation model *J. Atmosph. Sci.* **46** 1943–70

Spencer R W, Goodman H M and Hood R E 1989 Precipitation retrieval over land and ocean with the SSM/I: Identification and characteristics of the scattering signal *J. Atmosph. Ocean. Tech.* **6** 254–73

Szoke E J and Zipser E J 1986 A radar study of convective cells incmesoscale systems in GATE Part II: Life cycles of convective cells *J. Atmos. Sci.* **43** 199–218

Waliser D E and Graham N E 1993 Convective cloud systems and warm-pool sea surface temperatures: coupled interactions and self-regulation *J. Geophys. Res. Atmos.* **98** 12881–93

Webster P J and Stephens G L 1984 Cloud-radiation interaction and the climate problem *The Global Climate* ed J Houghton (Cambridge: Cambridge University Press) 63–78

Williams M and Houze R A 1987 Satellite-observed characteristics of winter monsoon cloud clusters *Mon. Wea. Rev.* **115** 505–19

Yuter S and Houze R A 1995 Three dimensional kinematic and microphysical evolution of Florida cumulonimbus part ii: frequency distributions of vertical velocity, reflectivity and differential reflectivity *Mon. Wea. Rev.* **123** 1941–63

Zipser E J, Liu C, Cecil D J, Nesbitt S W and Yorty D P 2006 Where are the most intense thunderstorms on earth? *Bull. Amer. Meteorol. Soc.* **87** 1057–71